

Deposition and characterization of Sb and Cu doped nanocrystalline SnO₂ thin films fabricated by the photochemical method

Dengbaoleer Ao*, Masaya Ichimura

Department of Engineering Physics, Electronics and Mechanics, Nagoya Institute of
Technology,

Gokiso, Showa, Nagoya 466-8555, Japan

*E-mail address:20516502@stn.nitech.ac.jp

Abstract: Sb-doped and Cu-doped SnO₂ thin films were deposited by the photochemical method. A solution containing SnSO₄ and a doping solution containing SbCl₃ or CuSO₄ were alternately dropped on the glass substrate and irradiated by the UV light. The Auger electron spectroscopy measurement revealed that Sb or Cu was contained in the deposited thin films. The dependence of electrical properties of the films on annealing temperature was studied. The Cu-doped SnO₂ thin film showed enhanced electrical conductivity after 400°C annealing in a nitrogen atmosphere.

Keywords: SnO₂, photochemical deposition (PCD), doping, resistivity

1. Introduction:

Tin dioxide SnO₂ is a wide band gap (3.6–3.8 eV) semiconductor and shows n-type conductivity without intentional doping. It is a technologically important material due to its various applications such as gas sensors, chemical sensors, and transparent conducting thin films. For most of those application, doping of impurities is needed to modify its conductivity, optical absorption and gas sensitivity.

Doped SnO₂ has been fabricated by various techniques, such as sol-gel[1-5], spray pyrolysis[6-8], and sputtering [9]. In our previous works, we deposited undoped and Pd-doped nanocrystalline SnO₂ thin films by a photochemical technique and applied them to hydrogen sensors [10-12]. In the photochemical deposition (PCD), an aqueous solution containing Sn²⁺ ions is irradiated by UV light, and SnO₂ is formed owing to photochemical reactions in the solution. The deposition process is easy and simple, and the apparatus is of very low cost. In the deposition, SnO₂ particles are formed in the solution and deposited on a substrate. Therefore, the films constitute of small particles, and the resulting high surface-to-bulk ratio is expected to enhance the number of sites for the gas reaction and thus enhance the sensitivity. For the hydrogen sensing, Pd is doped or coated on the SnO₂ film surface. The observed sensitivity was extremely high, i.e., the current increased by a factor of about 10³ for 50 ppm hydrogen at room temperature. However, one drawback of our hydrogen sensor is that the base resistivity is so high that the sensor is not compatible with conventional sensor system.

In this work, we attempt to establish the doping technique in PCD of SnO₂. Antimony Sb and copper Cu are selected as the impurity to incorporate into SnO₂. Sb is commonly used as a donor impurity for SnO₂. Cu is known to enhance sensitivity for H₂S of a SnO₂-based gas sensor[13].

Since PCD is a unique original deposition process, any doping study has not been reported so far. Once the doping technique is established, it can be utilized for various impurity elements to modify electrical and optical properties and also to control sensing characteristics of the SnO₂ films.

2. Experimental detail

Doped and undoped SnO₂ thin films were fabricated by the drop-photochemical deposition (drop-PCD) method. The SnO₂-deposition solution is an aqueous solution containing 10 mmol/L of SnSO₄ with the pH adjusted to 2.0 with HNO₃. For deposition of undoped SnO₂ films, a small amount of the SnSO₄ solution was dropped on the glass substrate and irradiated by the UV light, as shown in Fig. 1. The light source was an ultrahigh-pressure mercury arc lamp of 500 W, and the substrate area of about 1 cm² was irradiated through a spherical lens. One irradiation time was 5 min, and the substrate was washed with water and dried before the new solution was dropped on it. We obtained a SnO₂ film with a thickness of about 0.15 μ m by repeating the above process 10 times.

For impurity doping, a solution for the SnO₂ deposition and another solution for the doping were prepared separately. A small amount of each of these solutions was alternately dropped on the glass substrate, and irradiated by the UV light. In this process, a thin SnO₂ film is deposited in the first drop-irradiation cycle, and then in the next cycle, impurity atoms will replace some of the Sn atoms in the deposited films. The Sb doping solution is a 2-propanol solution containing 2 mmol/L of SbCl₃. For the Cu doping, the following two aqueous solutions were prepared. One is a solution including 2 or 20 mmol/L CuSO₄ (1). The other one is a solution containing 20 mmol/L CuSO₄ and 50 mmol/L Na₂SO₃ (2) with solution pH about 7.2 (unadjusted). We repeated the drop-irradiation cycles 20 times (10 times for the SnO₂ deposition and 10 times for the doping, alternately) and obtained doped SnO₂ thin films with a thickness of around 0.10~0.20 μ m. We confirmed that for both Sb and Cu, no film was deposited when only the doping solution was dropped and irradiated. The SnO₂ thin films were annealed in nitrogen ambient at 200°C, 300°C and 400°C.

The compositional analysis was carried out by Auger electron spectroscopy (AES) using the model JEOL JAMP 7800 Auger microprobe at probe voltage 10 kV and current 2×10^{-8} A. An argon-ion sputtering with acceleration voltage 3 kV and current 20 mA was used to sputter the film surface. The optical transmission measurement was performed using the JASCO U-570 spectrometer with the glass substrate as the reference. X-ray diffraction (XRD) was measured using Rigaku Smartlab diffractometer with Cu K radiation source. The surface morphology of the film was analyzed by scanning electron microscope (SEM; Hitachi S-3000H), keeping the acceleration voltage at 25 kV and magnification at 6000. In addition, indium electrodes (electrode size 1x1 mm²) were thermally evaporated and the current-voltage (I-V) characteristics were measured for the as-deposited as well as the annealed films. The conduction type was judged by the hot-probe method. The van der Pauw–Hall measurement was performed at room temperature for the 400°C annealed films using TOYO Corporation Model ResiTest 8310.

3. Results:

Figure 2 shows the AES spectra of the as-deposited SnO₂ thin films doped with Sb and Cu after 10 s Ar-ion sputtering. The solution containing 2 mmol/L CuSO₄ was used for the Cu doping. From those spectra, contents of impurity elements were evaluated using standard Auger efficiencies for elements. (The actual Auger intensity is known to depend on the matrix material and thus the following composition analysis could be regarded as an order-of-magnitude estimate.) The Sb/Sn atomic ratio in the film is as high as 0.53. In contrast, Cu content is relatively low, i.e., the Cu/Sn atomic ratio is about 0.08, when the solution containing 2 mmol/L CuSO₄ was used. The Cu content did not change significantly even when the CuSO₄ concentration in the doping solution was increased to 20 mmol/L. To enhance Cu content, solution (2) was used, i.e, 50 mmol/L Na₂SO₃ was added to the solution containing 20 mmol/L of CuSO₄. It was reported that the formation of the copper oxide is promoted by using the SO₃²⁻ ions as a reducing agent[14]. Thus, if the SO₃²⁻ ions act as a reducing agent in the PCD process, incorporation of Cu atoms into the film could also be promoted. However, the Cu/Sn atomic ratio was about 0.10, i.e., did not significantly increase compared with the case of solution (1).

From the optical transmission spectra shown in Fig. 3, it can be seen that the doped and undoped SnO₂ thin films have fairly high transnission in the visible region of the spectrum. The optical transmissions of all the samples except for Sb-doped SnO₂ are more than 80% in the visible region, whereas the transmission of the Sb-doped SnO₂ film is slightly lower than those of others. The optical band gap energy was calculated from the classical relation for direct-band optical adsorption.

$$\alpha = k(h\nu - E_g)^{1/2} / h\nu \quad (1)$$

where α is the absorption coefficient, k a constant, E_g the band gap and $h\nu$ the photon energy. Figure 4 shows the variation of $(\alpha h\nu)^2$ versus $h\nu$, which is linear in the higher energy domain, indicating a direct optical transition. The band gap energy E_g was obtained by extrapolating the linear portion of the graph to the energy axis at $\alpha = 0$. The obtained band gap values are around 3.7~3.8 eV for both the undoped and doped SnO₂ thin films.

Figure 5 shows the plots of resistivity for the undoped and doped samples annealed at different temperatures (the data for the as-deposited film were plotted at 27°C). The measured resistivity of the films deposited under the same condition shows scatter of about $\pm 10\%$, which will be due to nonuniformity of the film. The resistivity higher than $10^6 \Omega\text{cm}$ cannot be measured by our measurement system. Therefore, the electrical resistivity could be higher than $10^6 \Omega\text{cm}$ for the as-deposited films and the films annealed at 200 and 300 °C. The resistivity was decreased by the 400 °C annealing. The conduction type judged by the hot probe method was n-type for all the samples annealed at 400°C. The resistivity of the film was found to become significantly lower by the Cu doping, as shown in Fig. 5. Any further decrease in the resistivity of the Cu-doped SnO₂ was not seen when the concentration of Cu in the doping solution was increased from 2 mmol/L to 20 mmol/L. This is consistent with the AES results that the Cu content was not increased by increasing CuSO₄ concentration in the solution.

The carrier concentration and mobility were determined by the Hall measurements at room

temperature for the film annealed at 400°C. For the Cu-doped SnO₂ films (2mM CuSO₄), the results showed that the electron concentration is $3 \times 10^{16} \text{ cm}^{-3}$ and the carrier mobility $0.4 \text{ cm}^2 \text{ V}^{-1} \text{ s}^{-1}$. Since there is scatter of about $\pm 10 \%$ in the resistivity value, the same amount of scatter is expected for the Hall measurement results. The measurement failed for the undoped film because of its high resistivity.

Figure 6 shows the morphology of the as-deposited films. There is no apparent difference in morphology between the undoped film (Fig.(a)) and the Sb-doped film (Fig.(b)). The morphology of the Cu-doped SnO₂ thin films is shown in Figs. 6 (c) and (d). Grain structure can be seen more clearly for the Cu-doped films than for the undoped film.

For all the samples annealed at 400°C, XRD patterns were recorded, but we did not observe any clear peaks which can be attributed to the deposit.

4. Discussion

The Cu content in the Cu-doped films did not increase significantly even when the CuSO₄ content of the doping solution was increased. This result may be explained as follows. In the photochemical doping process of Cu, Cu atoms would replace the Sn atoms in the vicinity of the SnO₂ film surface during the photo-irradiation. Such photochemical doping of Pd into a SnO₂ film has been observed in our previous works [10-12]. In this process, only a limited number of Sn atoms in the vicinity of the surface may be available for the replacement, and thus once all of them are replaced by the impurity atoms, the replacement could not proceed further. Therefore, the Cu content in the film did not increase with increasing amount of CuSO₄ concentration in the solution. On the other hand, Sb content is considerably larger. This indicates that Sb atoms replaced not only the surface atoms but also Sn atoms in the bulk. Then, we can consider a possibility that an Sb-rich phase was formed in the film.

Sb is a group V element and thus can act as a donor if it substitutes Sn, which is a group IV element. However, in our experiment, the Sb doping did not result in decrease in resistivity. We can consider two reasons for this. The first one is the change in the film morphology. If the film becomes more porous, the observed resistivity will not be decreased. However, since there is no apparent change in the morphology compared with the undoped film, the morphology could not be the dominant factor. The second possible reason is that the Sb atoms did not replace Sn atoms but formed a separate high resistivity phase, probably Sb₂O₃. As discussed above, the AES results are considered to indicate the formation of Sb-rich oxide. For doping of Sb into the substitutional sites, formation of the separate phase needs to be suppressed by, for example, using a much more diluted SbCl₃ solution.

In contrast to Sb, substitutional Cu atoms in SnO₂ are not regarded as a donor since Cu has a smaller number of valence electrons than Sn. Copper oxide is conductive but usually shows p-type conductivity, and thus the observed decrease in resistivity will not be due to the formation of the copper oxide phase. One possible explanation of the reduced resistivity of the Cu-doped films is that the grain became larger due to the Cu doping. The growth of grain size will diminish effects of grain boundaries and reduce the resistivity. A few groups have reported deposition of Cu-doped

SnO₂ films so far. In ref.[8], it was reported that Cu doping leads to increase in grain size in spray pyrolysis deposited SnO₂ films, while in ref.[7], it was reported that Cu doping has minor effects on morphology and microstructure of the films obtained by electrostatic spray deposition. Electrical resistivity was not given in those previous papers. Our SEM results show that there are a larger number of grains for the Cu-doped films, but since the grains are separated from each other, they may not contribute to the electrical conduction. On the other hand, for all the samples annealed at 400°C, we did not observe any clear peaks in the XRD pattern. This indicates that increase in the grain size is not significant even after the annealing.

Another possible explanation for the resistivity reduction is that some portion of the doped Cu atoms are at interstitial sites. Cu⁺ or Cu²⁺ ions at interstitial sites will act as a donor and increase electron concentration. For the Cu-doped SnO₂ films annealed at 400°C, the Hall measurement results showed that the electron concentration is $3 \times 10^{16} \text{ cm}^{-3}$, and the carrier mobility $0.4 \text{ cm}^2 \text{ V}^{-1} \text{ s}^{-1}$. The mean free path estimated from the mobility is small, of the order of 0.01 nm, which is consistent with the fact that the grain growth is not significant according to the XRD results. Therefore, the enhanced conductivity will be mainly due to enhanced electron concentration, and thus the doped Cu atoms are thought to act as a donor. However, the Cu/Sn ratio determined from AES is about 0.1, which corresponds to a concentration much higher than the electron concentration. Thus the majority of the doped Cu atoms would be at substitutional sites, and only a small percentage of the Cu atoms are activated as a donor.

Conclusion

Sb-doped and Cu-doped SnO₂ thin films have been deposited on glass substrates using the PCD technique. The optical transmission of the film is fairly high in the visible region, and the band gap obtained is 3.7 - 3.8 eV. The resistivity of the 400°C annealed films is significantly lower for the Cu-doped film than for the undoped and Sb-doped films. The Hall measurement results show that the electron concentration is $3 \times 10^{16} \text{ cm}^{-3}$ for the Cu-doped SnO₂ films annealed at 400°C.

Acknowledgements:

We would like to thank Dr. M. Kato for his useful discussion and Prof. T. Egawa and Dr. K. Abe for their technical assistance.

References:

- [1] J.P. Chatelon, C. Terrier, E. Bernstein, R. Berjoan, J.A. Roger, Thin Solid Films 247 (1994) 162.
- [2] X. P. Cao, L. L. Cao, W. Q. Yao, X.Y. Ye, Thin Solid Films 317 (1998) 443.
- [3] Z. G. Ji, Z. J He, Y. L Song, K. Liu, Z. Z. Ye, J. Cryst. Growth 259 (2003) 282.
- [4] Y. Hu, S. -H. Hou, Mat. Chem. Phys. 86 (2004) 21.
- [5] T. N. Soitah, C. H. Yang, L. Sun, Mat. Sci. Semicond. Proc. 13 (2010) 125.

- [6] S. Shanthi, C. Subramanian, and P. Ramasamy, *J. Cryst. Growth* 197 (1999) 858.
- [7] C. M. Ghimbeu, R.C. V. Landschoot, J. Schoonman, M. Lumbrellas, *J. European Ceramic Soc.* 27 (2007) 207.
- [8] G. Korotcenkova, S. D. Hana, *Mat. Chem. Phys.* 113 (2009) 756.
- [9] T. Y. Yang, X.B. Qin, H. H. Wang, *Thin Solid Films* 518 (2010) 5542.
- [10] D. Ito, M. Ichimura, *Jpn. J. Appl. Phys.* 45 (2006) 7094.
- [11] M. Ichimura, T. Sueyoshi, *Jpn. J. Appl. Phys.* 48 (2009) 015503
- [12] M. Ichimura, Aodengbaoleer, T. Sueyoshi, *Phys. Status Solidi C7* (2010) 1168.
- [13] J. Tamaki, T. Maekawa, N. Miura, N. Yamazoe, *Sens. Actuators B* 9 (1992) 197.
- [14] M. Muhibbullah, M. Ichimura, *Jpn. J. Appl. Phys.* 49 (2010) 081102.

Figure captions:

Fig. 1 Schematic of the photochemical deposition apparatus.

Fig. 2 AES spectra of the doped SnO₂ thin films. Inset shows the expanded Cu-doped SnO₂ AES spectrum near the position of Cu peak.

Fig. 3 Optical transmission of the undoped and doped SnO₂ thin films.

Fig. 4 Plot of $(\alpha h\nu)^2$ against $h\nu$ of the undoped and doped as-deposited films.

Fig. 5 Resistivity of the various SnO₂ samples annealed at different temperatures.

Fig. 6 SEM images of the various as-deposited SnO₂ films: (a) undoped SnO₂; (b) Sb-SnO₂; (c) Cu-SnO₂ [2mM CuSO₄]; (d) Cu-SnO₂ [20mM CuSO₄ and 50mM Na₂SO₃].

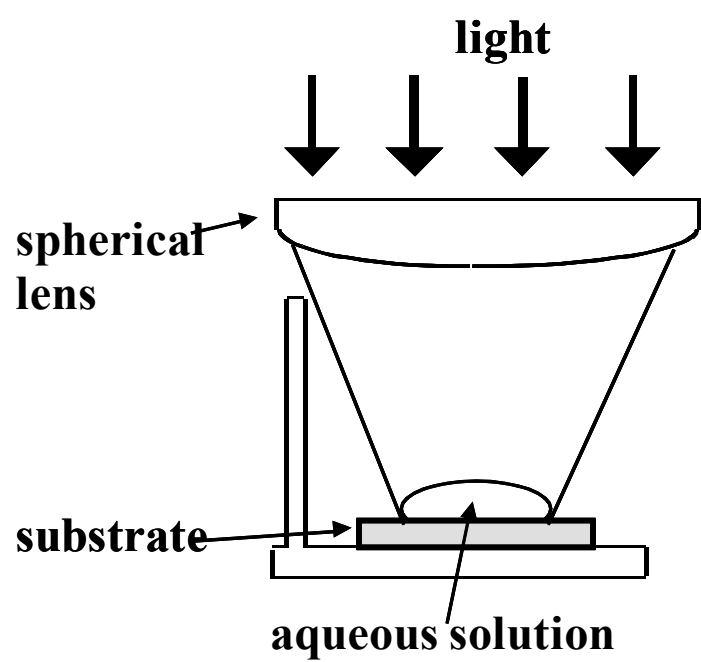


Fig. 1

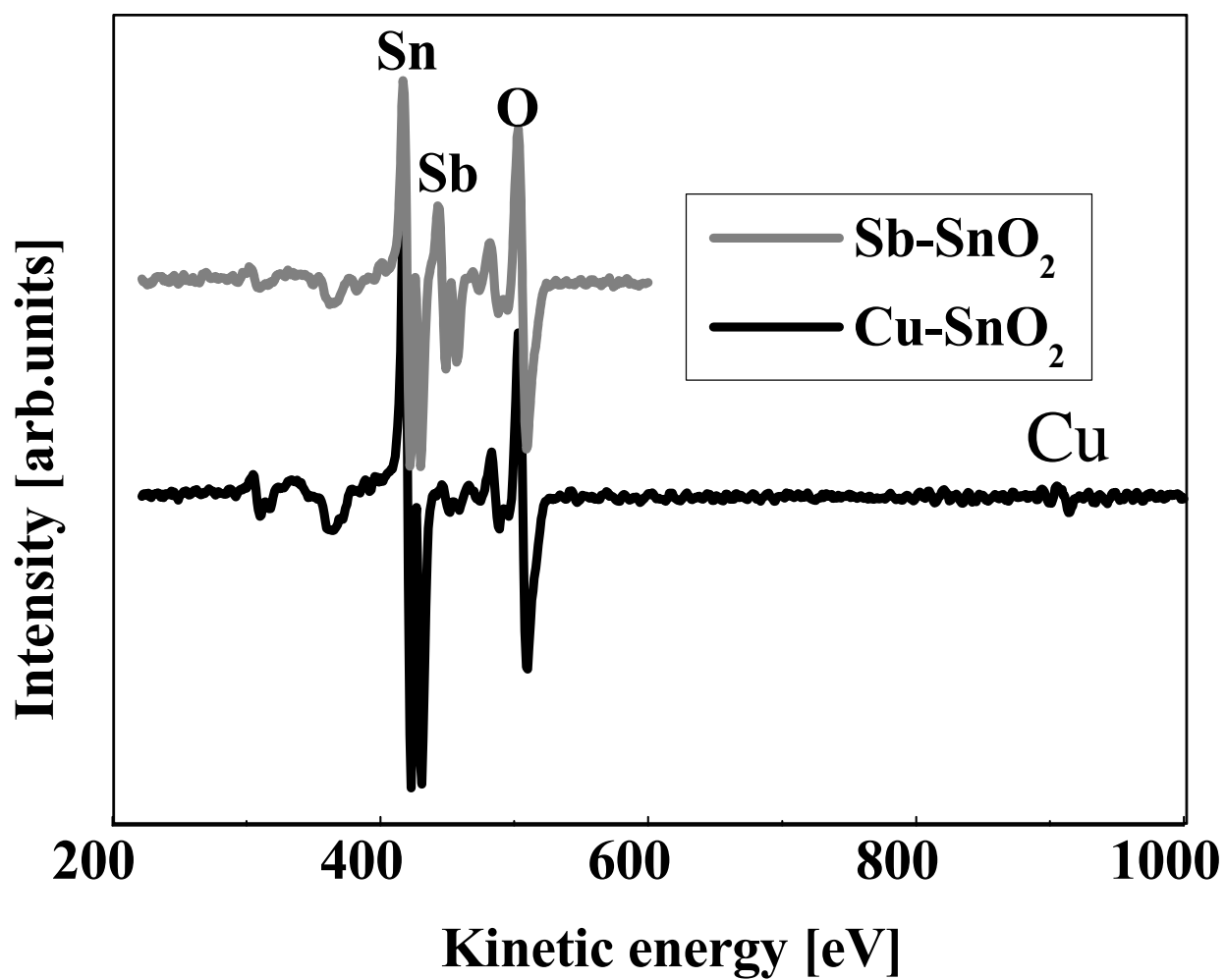


Fig. 2

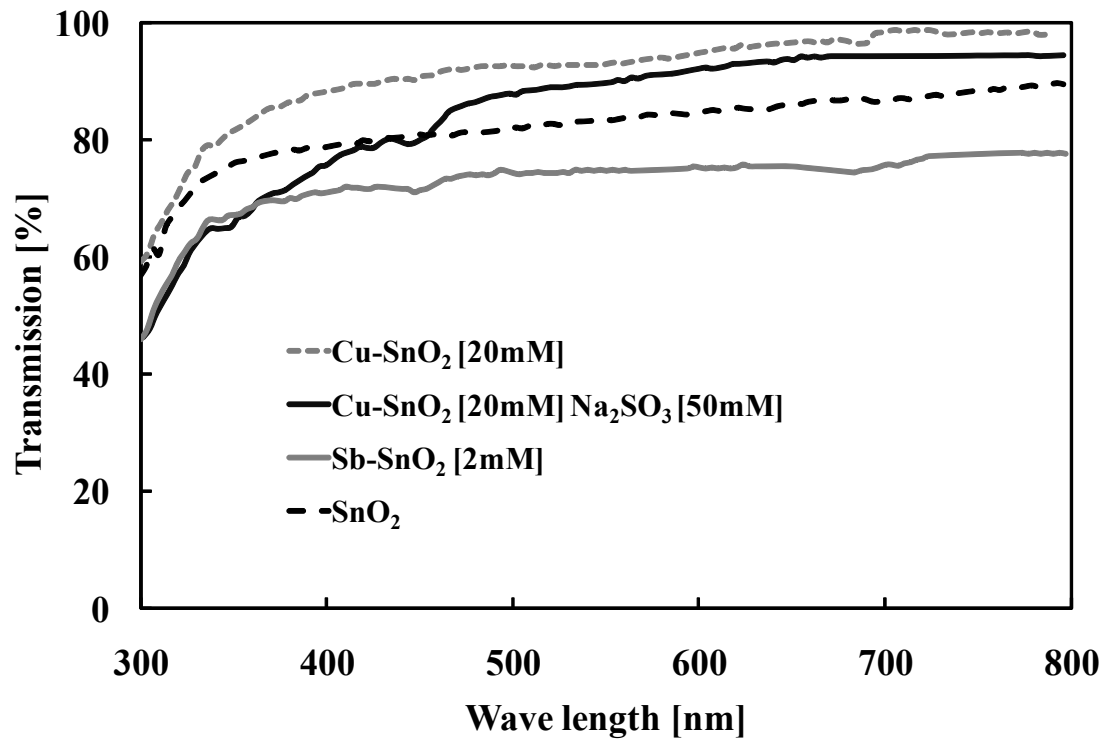


Fig. 3

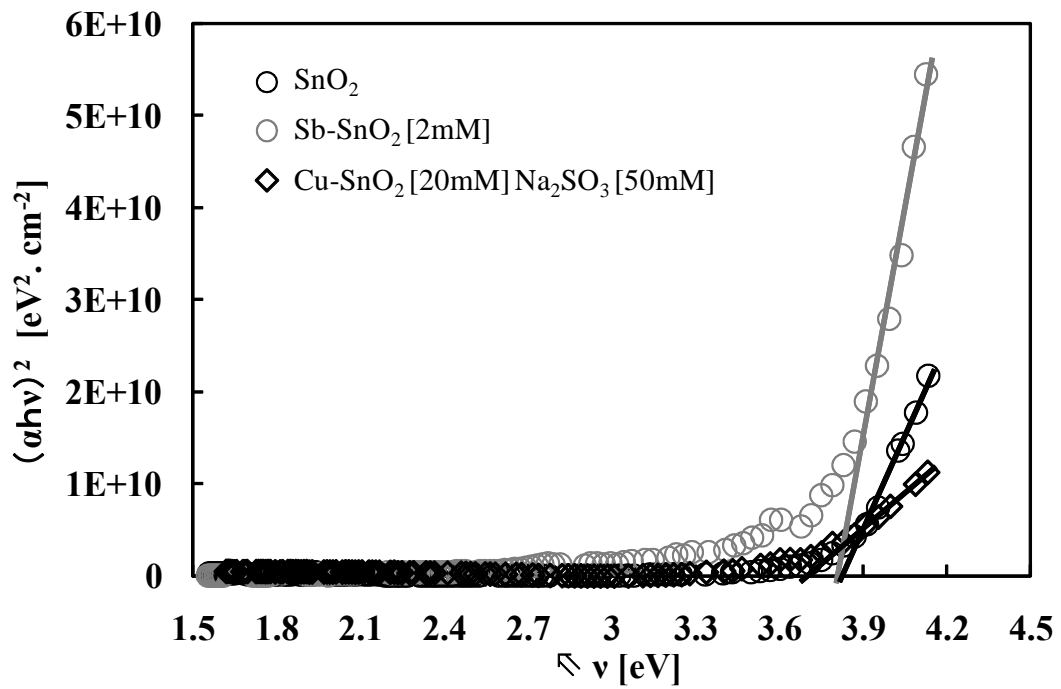


Fig. 4

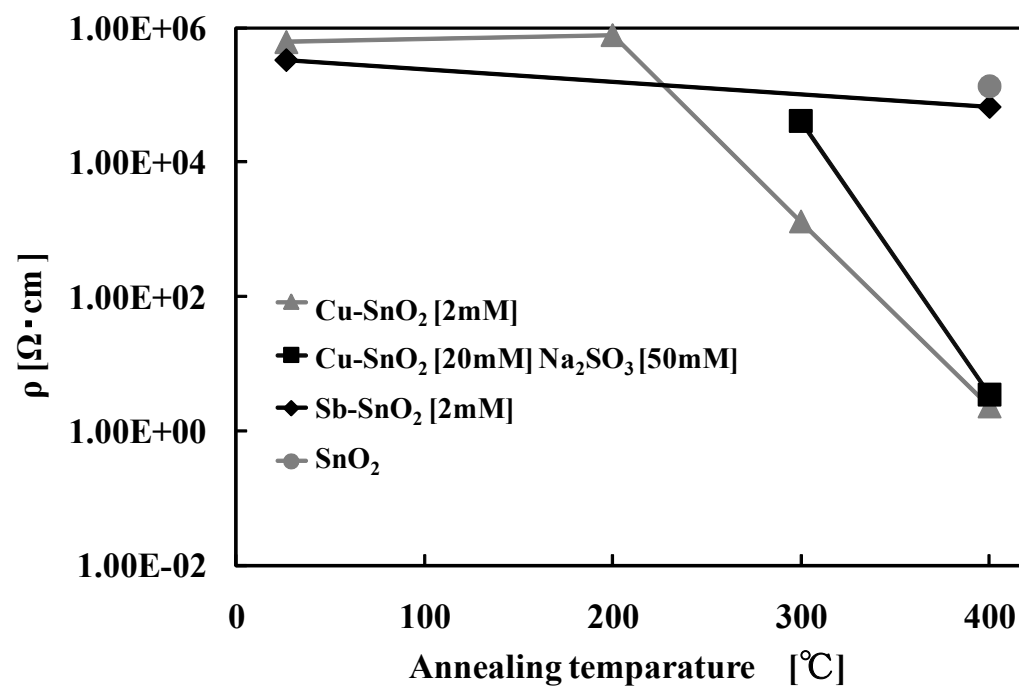


Fig. 5

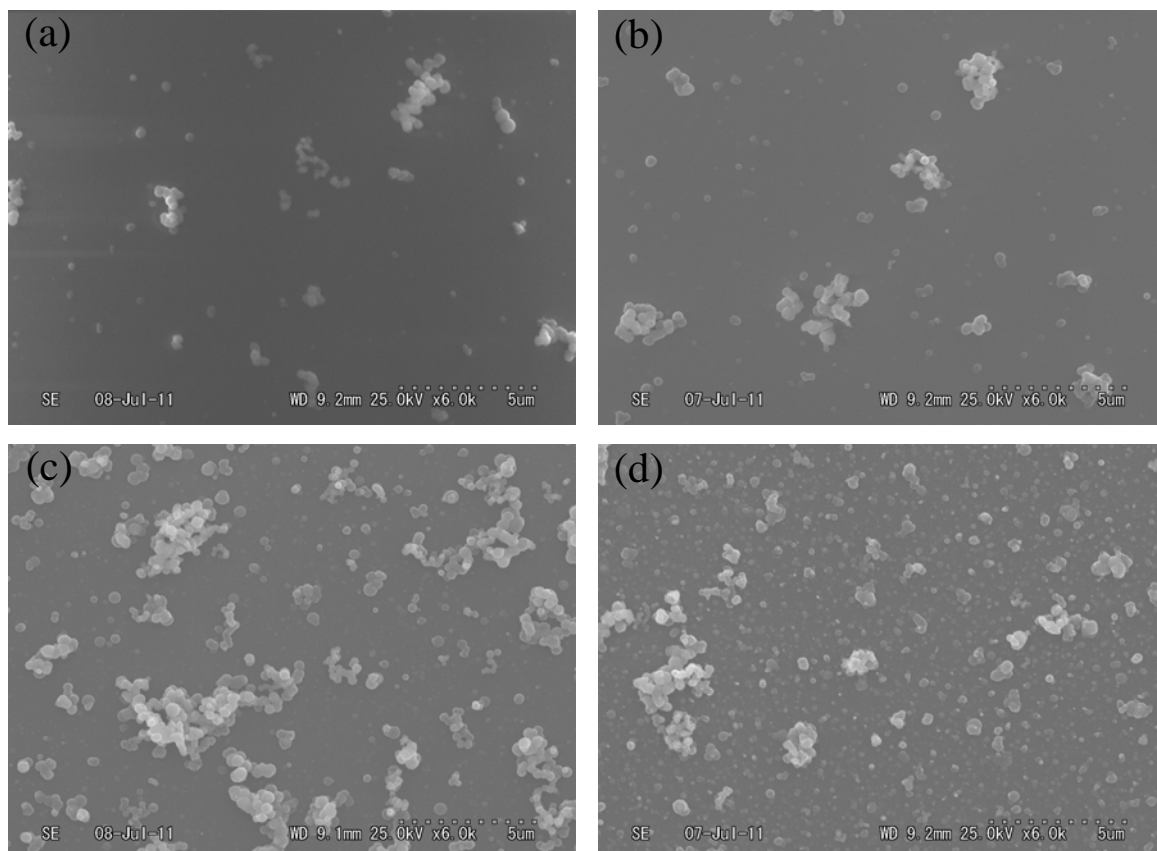


Fig. 6